eJSE INTERNATIONAL

Experimentally Investigating the Strengthening Effect of NSM-GFRP Bars on the Capacity of RC Slabs

Sama Taha[a], George Iskander[b]*, Mohamed Abou-Zeid[a], Ezzeldin Sayed-Ahmed[a]
[a] American University in Cairo, Egypt
[b] The University of Calgary, Alberta, Canada
*Corresponding author: george.iskander@ucalgary.ca

Abstract

This study aims to investigate the strengthening effect of GFRP bars on the capacity of RC slabs when subject to flexure loading. The objective is to show the effect of debonding failure on the capacity of the GFRP strengthened slabs relative to the different variables used. The variables used are different bonding lengths, diameters, and numbers of GFRP bars in strengthening RC slabs. The work presents the details of the adopted experimental investigation and the results of the flexural tests performed on twelve slabs with the different variables. These results are adopted to validate the currently available design provisions of the ACI code of practice for using NSM GFRP to strengthen RC slabs. The results showed that strength gain is directly proportional to the reinforcing ratio. However, the deflections of all strengthened and un-strengthened specimens did not significantly change.

Keywords

1. Introduction

Fiber Reinforced Polymers (FRPs) have been widely used to improve the structural performance of constructed reinforced concrete elements (Parvin et al., 2016). FRPs have several advantages compared to traditional steel reinforcement: they have a much higher strength to weight ratio (Parvin et al., 2016) and better fatigue properties (Behzard et al., 2016). When comparing FRP composites to steel, it was noticed that they are "unresponsive to the chloride-induce corrosion on account of its non-corrosive and non-metallic intrinsically" (Abbood et al., 2020).

There are many different types of FRP: Carbon (CFRP), Glass (GFRP), Aramid (AFRP) and Basalt (BFRP). Despite not being the strongest FRP option, GFRP remains an attractive choice due to its cost-efficiency and moderate levels of strength and stiffness (Xing et al., 2018).

There are different techniques to strengthen Reinforced Concrete (RC) elements with FRP, the most common of which are the Externally Bonded (EB) technique and the Near-Surface Mounted (NSM) technique.

Fig. 1 shows the EB technique in which sheets of FRP are bonded to the external surface of the RC element. In NSM technique, a small groove is cut in the surface of the RC element in consideration in which an FRP bar is placed and bonded (Parvin et al., 2016).

FRP strengthening with the NSM technique has two key advantages in comparison to the EB technique: NSM is far less susceptible to debonding (owing to the increased bond surface area created by the groove) and is typically faster and easier to install in the field (Coelho et al., 2015). The adhesive which covers the bars in the NSM technique also acts to protect the reinforcement from aggressive environmental factors. Consequently, NSM allows for more efficient and robust use of FRP.

Like any FRP strengthening technique, the success of NSM hinges on establishing adequate bond between the FRP and the surrounding concrete; premature debonding will result in an ineffective intervention and an in-situ strength far below design calculations. Hence, the increase in strength of RC elements strengthened using GFRP bars may be limited by this premature debonding failure mechanism. Lately, the necessity of studying the increase in strength and the different modes of failure when strengthening RC elements with FRP bars is increasing. As well as studying the different bonding lengths, to reach the maximum possible strength without debonding failure, to be able to benefit from the various advantages of using FRP materials (Basaran and Kalkan, 2020).

This work aims to investigate the effect of the diameter, volume, and numbers of GFRP bars (i.e., reinforcement ratio) on the flexural strength of concrete slabs. This research also studies the adequacy of ACI's NSM development length provisions in preventing debonding failure, as well as the accuracy of its strength predictions, for NSM GFRP strengthened slabs.

As per the ACI Code (ACI, 2008), the minimum dimension of the groove for the NSM technique is equal to 1.5 multiplied by the FRP bar diameter, to make sure enough adhesive fills the groove and covers the FRP bar. Therefore, the minimum dimension of the groove (h_g & t_g) is 12 mm, 18 mm and 24 mm for 8 mm, 12 mm, and 16 mm bar diameters, respectively. Thus, a groove dimension of 20 × 20 mm was used for 8 mm and 12 mm bars, and a groove dimension of 25 × 25 mm was used for 16 mm bars.

Moreover, ACI 440.R2.2008 has a minimum dimension for the FRP bar bonding length to mitigate premature debonding failure. The purpose for having a limit for the bonding length is to delay the failure of the GFRP bar by detaching from the concrete. Eq. (1) is used to calculate the minimum bonding length for the FRP bar (l_{db}) for the different used diameters. This equation is derived from equating the force applied on the bar which is equal to $A_f \times f_{fd}$, to the circumference of the bar in contact with the RC which equals to $\tau_b \times l_{db} \times \pi d$.

$$l_{db} = \frac{d_b}{4(\tau_b)} f_{fd} \tag{1}$$

where, A_f is the area of one bar, d_b is the used GFRP bar diameter, τ_b is the design value bond strength and f_{fd} is the short-term tensile stress.

By applying Eq. (1), the minimum l_{db} is 811 mm, 1095 mm and 1298 mm for 8 mm, 12 mm, and 16 mm bars, respectively.
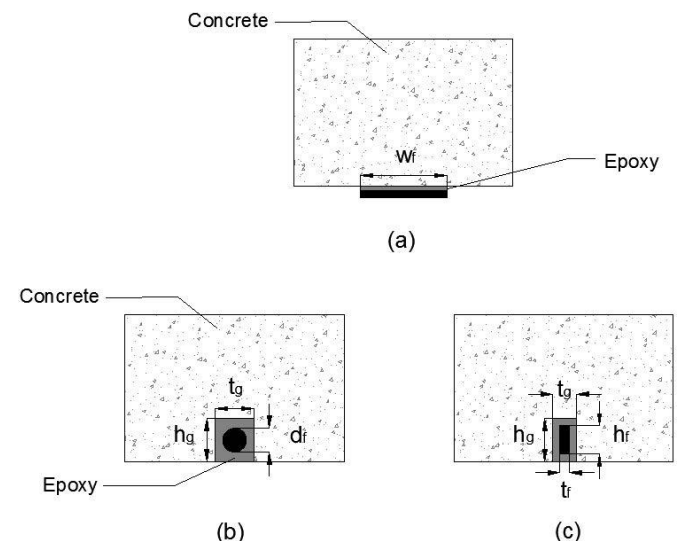
Fig. 1 FRP strengthening (a) EBR FRP plate or sheet, (b) NSM FRP rod or bar, (c) NSM FRP laminate (Parvin et al., 2016).

2. Experimental Program

Six sets of two slabs (for a total of twelve) were built and tested in the AUC structural engineering lab. Detailed dimensions are provided in Fig. 2, and a summary of the characteristics of each set is provided in Table 1. The first set (S1) served as a control, consisting of two slabs with 10M reinforcing bars @ 200 mm and no NSM-GFRP bars. All subsequent sets had the same steel reinforcement as S1, but varying NSM-GFRP configurations. Sets S2, S3 and S4 tested the inclusion of a single NSM-GFRP bar of constant bonding length (2.0 m) but varying diameter to test the effect of the GFRP diameter: S2 was strengthened with one 12M GFRP bar; S3 with one 8M GFRP bar; and S4 with one 16M GFRP bar. Set S5 was strengthened with one 12M GFRP bar, but the bonding length was cut to 1.0 m (below the ACI limit) to examine the behaviour of a specimen with insufficient bonding length according to the ACI. Set S6 was strengthened with two 12M GFRP bars with a bonding length of 1.5 m to investigate the effect of increasing the reinforcement ratio used in the strengthening operation. Since, the ACI minimum bond length for GFRP bars with 8 mm, 12 mm, and 16 mm diameters, is 811 mm, 1095 mm, and 1298 mm, respectively, the used length will be 2.0 m for series with GFRP bars of no. 8 and no. 12 mm, which is greater than the accepted minimum, as the focus for these 3 series is analyzing the effect of using GFRP with different diameters. Moreover, the bonding length will be tested as a variable for series with GFRP bars of no. 16 mm where 3 different dimensions will be used equal to 1.0 m, 1.5 m, and 2 m, which are less, approximately equals to and greater than the calculated minimum, to be able to analyze the effect of the bonding length on the flexural capacity.
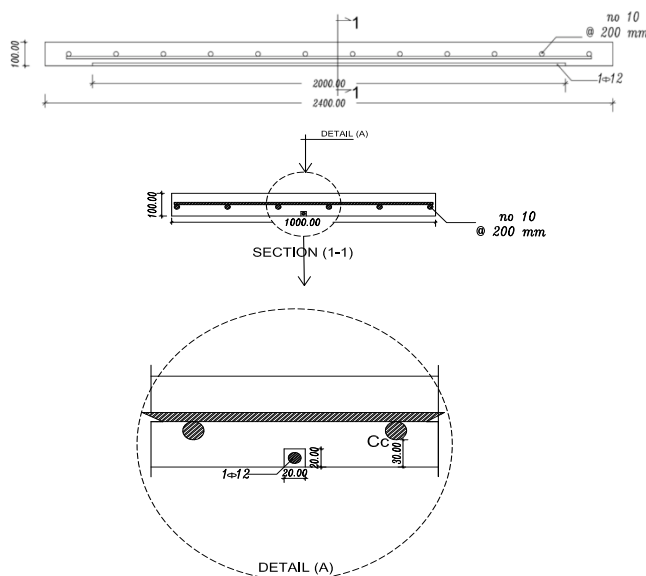
Fig. 2 Series 1 cross-section drawings

Series	No. of slabs	Slabs dimensions (m)	Groove (mm)	GFRP length (m)	# of GFRP bars	GFRP dia. (mm)
S1	2	1.0×2.4×0.1	-	-	-	-
S2	2	1.0×2.4×0.1	20 × 20	2.0	1	12
S3	2	1.0×2.4×0.1	20 × 20	2.0	1	8
S4	2	1.0×2.4×0.1	25 × 25	2.0	1	16
S5	2	1.0×2.4×0.1	25 × 25	1.0	1	16
S6	2	1.0×2.4×0.1	25 × 25	1.5	2	16

One batch of ready-mix concrete was used to cast the twelve specimens. 12 (150 × 150 × 150 mm) sample cubes were cast from the same mix. The cubes were tested, and the 28-days compressive strengths was 36 ± 3.4 MPa. The average Young's Modulus of elasticity of the cubes was 27,800 MPa and the ultimate strain is 0.003. The used steel has a 360 MPa yield stress and 200,000 MPa Young's Modulus of elasticity.

The GFRP bars were obtained from Schoeck Bauteile GmbH (Germany). Straight ComBAR GFRP bars are certified worldwide and are following ACI 440.R2 (Schoeck, 2018). As per the Schoeck Combar material manual, the GFRP bars have a tension modulus of elasticity equal to 60,000 MPa, compressive modulus of elasticity is 80% of E (i.e Ec is equal to 48,000 MPa). The design value bond strength is equal to 3.7 MPa and the tensile strength depends on the bar diameter ranging from 1200 to 1500 MPa. (Schoeck, 2018).

The slabs were tested in a displacement control protocol under three-point bending, as shown in Fig. 3. The load was applied on a 1 m loading beam gradually using an Enerpac 100-ton hydraulic jack and was

monitored over the course of the test using a load cell. Three LVDTs were used to measure deflection. As shown in Fig. 3, LVDT 1 is located at the top of the concrete surface, LVDT 2 located at the midspan to measure the maximum deflection and LVDT 3 below the beam used as a support, to monitor its movement. Strain gages were applied to the concrete top and bottom surfaces to measure the concrete strain in compression and in tension. Strain gauge arrangement is shown in Fig. 3 where strain gauge 1 is 10×10 mm² and is placed on the steel reinforcement primary bar in the middle of the sample, strain gauge 2 is 30×30 mm² and is placed at the top surface of concrete to measure the concrete's strain in compression, strain gauge 3 is 60×60 mm² and is placed at the bottom surface of concrete, to measure the concrete's strain in tension, strain gauge 4 is 30×30 mm² and is placed at the epoxy surface to measure any movement in relevance to the GFRP, strain gauges 5 and 6 are 6×6 mm² and 10×10 mm² and are placed on the 8 mm and 12 and 16 mm bars, respectively.

3. Results and Discussion

Table 1 shows a summary of the following results for each sample: the experimental failure moment, the failure mode, and the ratio between the experimental failure moment to the control sample. Figs 4 to 9 show the failure mode, and the load strain curves for each series. Before testing Series 4 Sample 2, a concrete block fell on it causing minor damage. However, it was repaired using Grout and was tested. Figs 10 and 11 show the load displacement graphs for series 1 to 6.
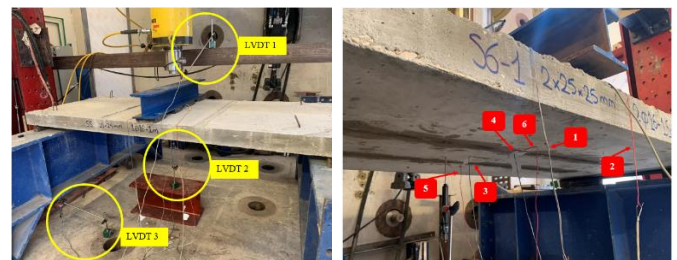
Fig. 3 Test Setup showing LVDT (left) and strain gauge locations (right)
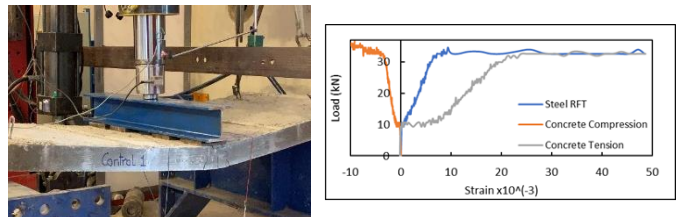
Fig. 4 Series 1 sample 1 failure and load strain graph
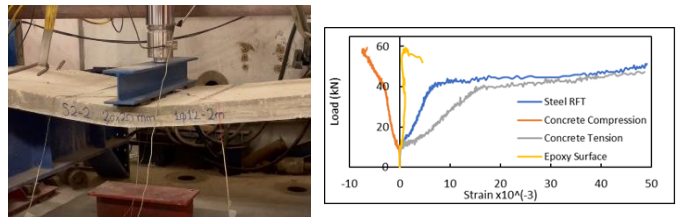
Fig. 5 Series 2 sample 2 failure and load strain graph
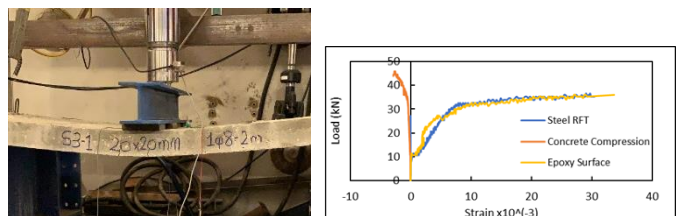
Fig. 6 Series 3 sample 1 failure and load strain graph
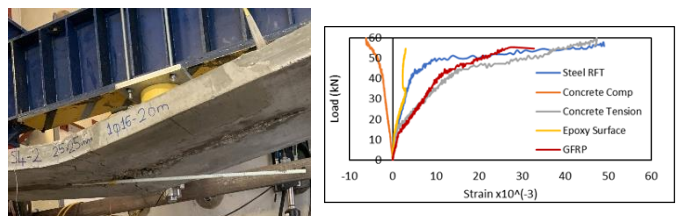
Fig. 7 Series 4 sample 2 failure and load strain graph
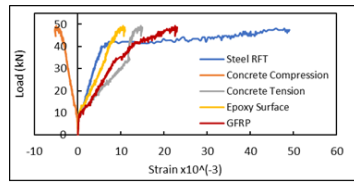
Fig. 8 Series 5 sample 1 failure and load strain graph
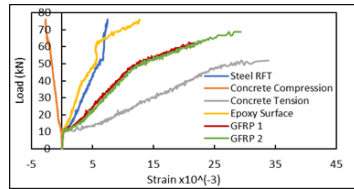
Fig. 9 Series 6 sample 1 failure and load strain graph

Table 1 Results summary

Sample	GFRP bars	Exp. M_f (kN·m)	Exp. Failure Mode	$\dfrac{M_{experimental}}{M_{control}}$
S1-1	Control	17.6	Flexural steel yielding	100%
S1-2	Control	17.1	Flexural steel yielding	100%
S2-1	1 no.12-2m	22.0	Flexural steel yielding	127%
S2-2	1 no.12-2m	22.0	Flexural steel yielding	127%
S3-1	1 no.8-2m	18.7	Flexural steel yielding	108%
S3-2	1 no.8-2m	20.4	Flexural steel yielding	117%
S4-1	1 no.16-2m	23.7	Flexural steel yielding	137%
S4-2	1 no.16-2m	27.5	Debonding	159%
S5-1	1 no.16-1m	25.9	Concrete crushing	149%
S5-2	1 no.16-1m	22.0	Concrete crushing	127%
S6-1	2 no.16-1.5m	34.7	Debonding	200%
S6-2	2 no.16-1.5m	35.8	Debonding	206%
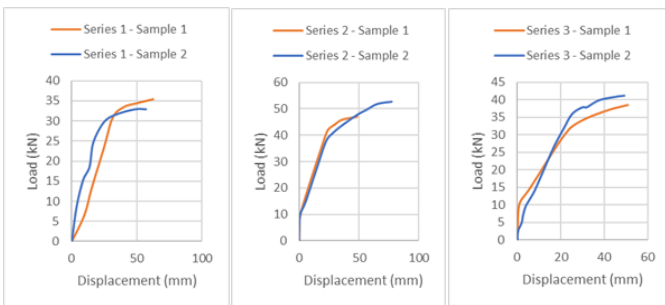
Fig. 10 Series 1 to 3 load displacement graphs (Engauge Digitizer Software)
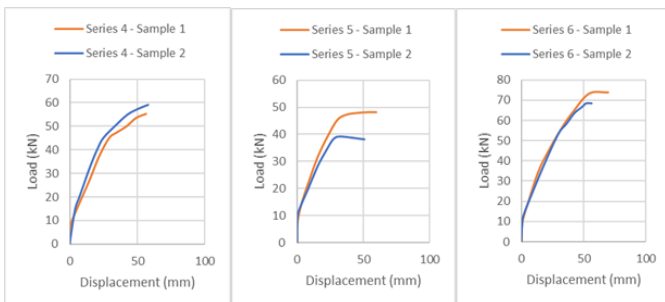
Fig. 11 Series 4 to 6 load displacement graphs (Engauge Digitizer Software)

4. Analysis and Summary

Comparing ACI's Provisions to the Experimental Results

As per ACI 440-R-08 2008, the failure load for the control samples was calculated using force equilibrium and strain compatibility. After that, the corresponding bending moment at failure was calculated. Table 3 shows the comparison between the calculated failure moments and the predicted mode of failure with the experimental findings.

The percentages of strength enhancement are calculated for the 6 groups and presented in Fig. 12. As shown in the Fig., series 2, 3, 4, 5 and 6 have a 27%, 13%, 48%, 38% and 103% strength increase when compared to the control specimen. This proves the efficiency of strengthening using NSM GFRP bars, even when there was premature debonding in series 5, there is an increase in moment.

Table 2 Comparison Summary

Series	ACI Failure Moment (kN·m)	ACI Predicted Failure Mode	Exp. Failure Moment (kN.m)	Exp. Mode of Failure
S1	12.98	Flexural	17.35	Flexural steel yielding
S2	24.21	Debonding	22.00	Flexural steel yielding
S3	17.12	Debonding	19.55	Flexural steel yielding
S4	33.17	Debonding	25.60	Flexural steel yielding, Debonding
S5	33.17	Debonding	23.95	Concrete crushing
S6	54.30	Concrete Crushing	35.25	Debonding

As shown in Fig. 13, the calculated failure loads for series 1 and series 3 are lower than the actual failure load. his is due to differences in the dimensions, workmanship, or steel reinforcement yield strength. However, since for series 3 the comparison to series 1 showed an increase in strength lower than the calculated increase in strength as per ACI equations, it shows that the calculations are underestimated for no.8 GFRP bar diameter.

However, for Series 4, 5 and 6 the calculated failure load is more than the actual failure load, which means that the code design equations are overestimated for no.16 GFRP bar diameter and for the series where the used bonding length is less than the minimum bonding length, this is due to their rapid premature failure due to debonding. As in series 5 the bonding length is equal to the minimum bonding length set in the code and in series 6 the bonding length is less than the minimum bonding length set in the code.
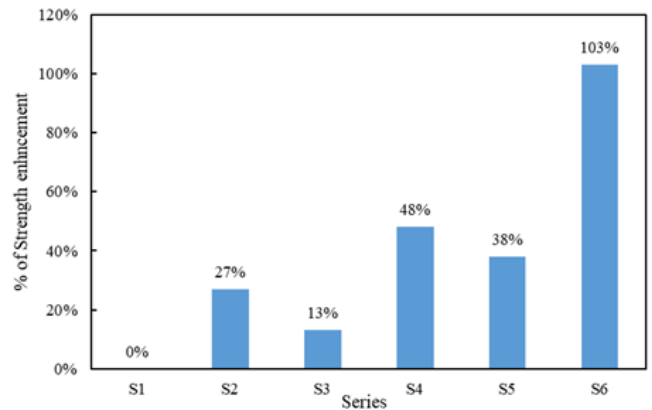
Fig. 12 Percentage Increase in Experimental Moment from Control Sample Moment

The GFRP reinforcement ratio is calculated for each sample, where the GFRP reinforcement area is divided by the concrete sample area. The higher the GFRP reinforcement ratio, the higher increase in failure load with a linear behavior as shown in Fig. 14.
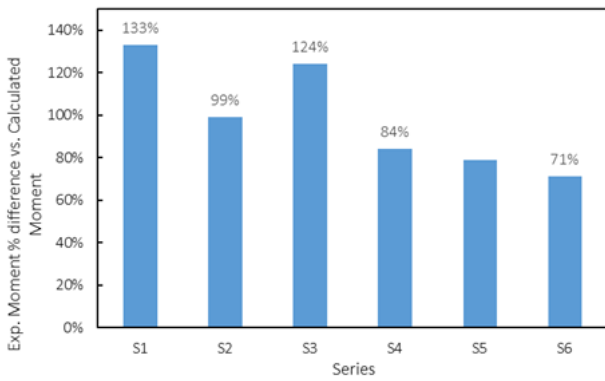
(a)
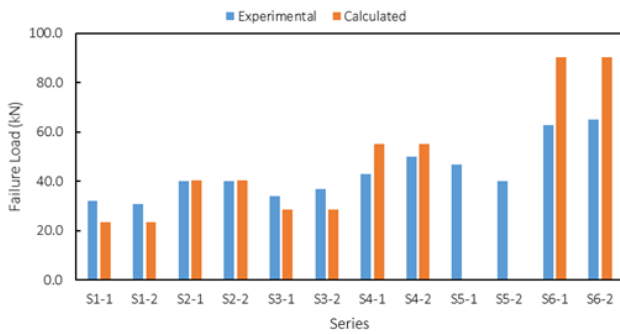
(b)

Fig. 13 (a) The ratios between experimental and ACI's failure moments. (b) A comparison between actual and calculated failure loads
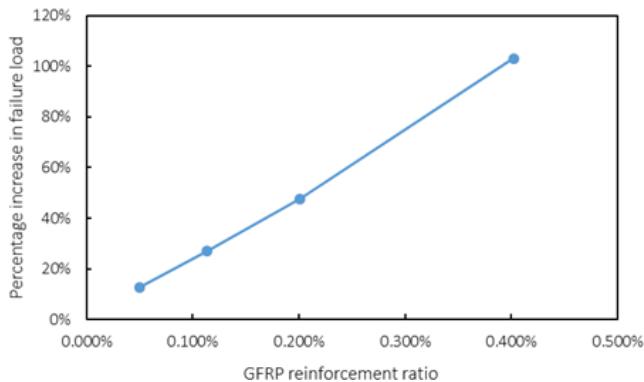
Fig. 14 Percentage increase in failure load (P_f) vs. GFRP reinforcement ratio

The GFRP development length to the GFRP bar diameter is calculated. The higher the GFRP length to diameter ratio, the lower the increase in failure load as shown in Fig. 15.

However, for the series with the lowest length to diameter ratio equal to 62.5 and development length 1000 mm, the percentage increase was lower than series with higher length to diameter ratio. As its development length is smaller than the minimum specified by the code and its mode of failure was due to debonding.
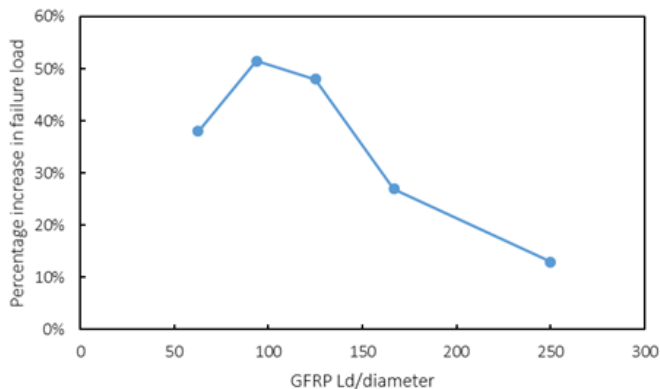
Fig. 15 Percentage increase in failure load vs. the GFRP development length to diameter

5. Conclusion

Considering the materials used, sample design, steps of execution and test parameters associated with this study, the following conclusion can be stated:

Strengthening of RC Slabs using NSM GFRP showed a significant increase in strength and load carrying capacity. Where no. 8 increased the load by 13%, no. 12 by 27% and no. 16 by 48%.

Given a constant number of bars, the larger the GFRP bar diameter, the higher the strength of the RC slab.

The volume and reinforcement ratio of the GFRP bars used is proportional to the increase in strength.

ACI NSM GFRP code is accurate for length to bonding length greater than the minimum. As the mode of failure was due to flexural failure, the calculated failure load was less than the experimental for GFRP diameter no.8, equals to the experimental for GFRP diameter no.12 and was less than the experimental for GFRP diameter no.16.

ACI NSM GFRP code is unconservative for length to bonding length equal to the minimum. As the mode of failure was due to debonding of the GFRP bars and the calculated failure load was more than the experimental load.

The displacement of the specimens was an average of 57.6 mm vs. an average displacement of 60 mm for the control specimen. There is no specific pattern for the decrease and increase in displacement due to the use of GFRP. It needs further testing.

References

Abbood, Imad S., Odaa, Sief aldeen, Hasan, Kamalaldin F. and Jasim, Mohammed A., "Properties evaluation of fiber reinforced polymers and their constituent materials used in structures – A review", Materials Today: Proceedings, July 2020.

ACI Committee 440.2. "Guide For the Design and Construction of Externally Bonded FRP Systems for Strengthening Concrete Structure". ACI American Concrete Institute. 2008.

Aydin, F., and M. Saribiyik. "Compressive and Flexural Behavior of Hybrid Use of GFRP Profilewith Concrete." International Symposium on Sustainable Development. Materials Science. 2010.

Basaran, B. and Kalkan, I. "Development length and bond strength equations for FRP bars embedded in concrete". Composite Structures, Volume 251, 2020.

Behzard, Pejman, Sharbatdar, Mohammad and Kheyroddin, Ali. "Different NSM FRP technique for strengthening of RC two-way slabs with low clear cover thickness". Scientia Iranica. 23. 2016.

Bilotta, Antonio, Ceroni, Francesca, et al. "Bond of NSM FRP-Strengthened Concrete: Round Robin Test Initiative". Journal of Composites for Construction, American Society for Civil Engineering. 2015.

Carolin, Anders. "Carbon Fibre Reinforced Polymers for Strengthening of Structural Elements." Luleå University of Technology, Department of Civil, Environmental and Natural Resources Engineering., Luleå Tekniska Universitet, 2003.

Coelho, Mário, Sena-Cruz, Jose and Neves, Luis. "A review on the bond behavior of FRP NSM systems in concrete". Construction and Building Materials. 93. 2015.

De Lorenzis, Laura, Nanni, Antonio and La Tegola, Antonio. "Strengthening of Reinforced Concrete Structures with Near Surface Mounted FRP Rods". International Meeting on Composity Materials, PLAST 2000. 2000. Italy.

De Lorenzis, Laura and Teng, J.G. "Near-Surface Mounted FRP Reinforcement: An Emerging Technique for Strengthening Structures". Composites Part B: Engineering. 2007.

El-Hacha, Raafat and Rizkalla, S.H. "Near-surface-mounted fiber-reinforced polymer reinforcements for flexural strengthening of concrete structures". ACI Structural Journal. 101. 2004.

Engauge Digitizer Software. December 2021

Gunaslan, Sultan Erdemlı, and Abdulhalim Karasin. "Confining Concrete Columns with FRP Materials." European Scientific Journal, ISSN: 1857 – 7881, Apr. 2017, pp. 464–470. Accessed on 2, May 2021.

Hosen, Md Akter, U. Johnson Alengaram, Mohd Zamin Jumaat and N. H. Ramli Sulong, Kh. Mahfuz ud Darain. "Glass Fiber Reinforced Polymer (GFRP) Bars for Enhancing the Flexural Performance of RC Beams Using Side-NSM Technique." Polymers vol. 9,5 180. 19 May. 2017.

Hsieh, Chia-Tsung and Lin, Yiching, "Detecting debonding flaws at the epoxy–concrete interfaces in near- surface mounted CFRP strengthening beams using the impact–echo method" NDT&E International. May 2016.

Kang, T.HK., Howell, J., Kim, S. et al. A State-of-the-Art Review on Debonding Failures of FRP Laminates Externally Adhered to Concrete. Int J Concr Struct Mater 6, 123–134 (2012). https://doi.org/10.1007/s40069-012-0012-1.

Makhlouf, Aly. Kareem Mostafa, Sarah Rezk, Seif Eteifa and Ziad El Abd. "Testing Near-Surface Mounted Reinforcement in Concrete Using

Glass Fibre-Reinforced Polymer". American University in Cairo. Department of Construction Engineering. Supervised by Dr. Ezzeldin Yazeed and Dr. Mohamed AbouZeid. 2015.

Mohamedien, Mohamed A., Hosny, Abdel-Hady and Abdelrahman, Amr. "Use of FRP in Egypt, Research Overview and Applications". Procedia Engneering 54 2-21, 2013.

Parvin, Azadeh and Taqiuddin Syed Shah. "Fiber Reinforced Polymer Strengthening of Structures by Near-Surface Mounting Method." Polymers: 1-4. 2016.

Pultron Composites. "World's Largest GFRP Rebar Project Embraces Corrosion-Free Future." Pultron Composites. 13 Aug. 2019, www.pultron.com/composite-blog/worlds-largest-gfrp-project/

Salman, Wissam. "Strengthening of Reinforced Concrete One-Way Slabs with Opening using CFRP Strips in Flexural". International Journal of Science and Research (IJSR) Volume 4 Issue 5. May 2015.

Sathishkumar, TP., Satheeshkumar, S. and Naveen, J. "Glass fiber-reinforced polymer composites – a review". Journal of Reinforced Plastics and Composites. Vol. 33 (13) 1258–1275. 2014.

Schoeck ComBAR Brochure and Properties. August 2018. Accessed on 19, September 2019.

Schoeck ComBAR Technical Information. 2018.

Soliman, Shehab M., El-Salakawy, Ehab and Benmokrane, Brahim. "Flexural behaviour of concrete beams strengthened with near surface mounted fibre reinforced polymer bars". Canadian Journal for Civil Engineering Vol. 37. 2010.

Soror, A. Y., et al. "State of the Art Review: Flexural Strengthening of Reinforced and Pre-Stressed Concrete Beams Using Fiber Reinforced Polymers." Engineering Research Journal, vol. 42, no. 2, Apr. 2019.

Szabó, Zsombor and Balázs, György. "Near surface mounted FRP reinforcement for strengthening of concrete structures". Periodica Polytechnica-civil Engineering. 2007.

Xing, Guohua, Chang, Zhaoqun and Ozbulut, Osman. "Behavior and failure modes of reinforced concrete beams strengthened with NSM GFRP or aluminum alloy bars". 2018.